

Reaction Efforts Associated with Non-Holonomic and Rheonomic Constraints in Index-3 Augmented Lagrangian Formulations

Francisco González¹, Daniel Dopico², Javier Cuadrado³, József Kövecses¹

¹ Centre for Intelligent Machines and Department of Mechanical Engineering, McGill University. 817 Sherbrooke St. West, Montréal, Québec, H3A 0C3, Canada: franglez@cim.mcgill.ca, jozsef.kovecses@mcgill.ca

² Department of Computer Science and Department of Mechanical Engineering, Virginia Tech. 2200 Kraft Drive, Blacksburg, VA, 24060, USA: ddopico@vt.edu

³ Laboratorio de Ingeniería Mecánica, University of La Coruña. Mendizábal s/n, 15403 Ferrol, Spain: javicua@cdf.udc.es

Abstract

Index-3 augmented Lagrangian formulations with projections of velocities and accelerations represent an efficient and robust method to carry out the forward-dynamics simulation of multibody systems. They are currently used in a wide variety of applications, ranging from biomechanics to heavy machinery simulators. Existing formalisms, however, are only able to deal with kinematic constraints whose expression at the position level is known. When this expression is not available, e.g. when non-holonomic constraints enter the picture, the constraint reaction forces yielded by these algorithms are not correct anymore because they are obtained as a function of the violation of the constraints at position level alone.

In this work, a method to determine the constraint reaction forces from the expression of the projection of velocities and accelerations is introduced. The method was tested in the forward-dynamics simulation of a set of simple examples. Results showed that the proposed strategy can be used to expand the capabilities of the index-3 augmented Lagrangian algorithms, making them able to tackle kinematic constraints defined at the velocity level and provide the correct reaction efforts when non-holonomic constraints are used to model a mechanical system.

Keywords: *Multibody system dynamics, index-3 augmented Lagrangian method, projections of velocities and accelerations, velocity-level constraints, non-holonomic constraints, reaction efforts*

1 Introduction

The motion of mechanical systems subjected to kinematic constraints is often described with a set of differential algebraic equations (DAE's). Let us assume that a multibody system represented by a set of n generalized coordinates \mathbf{q} is restrained by m constraints that can be expressed in terms of the generalized coordinates as

$$\Phi(\mathbf{q}, t) = \mathbf{0} \quad (1)$$

Differentiation of Eq. (1) with respect to time yields

$$\dot{\Phi} = \Phi_{\mathbf{q}}(\mathbf{q}, t) \dot{\mathbf{q}} + \Phi_t(\mathbf{q}, t) = \mathbf{0} \quad (2)$$

where $\Phi_{\mathbf{q}} = \partial\Phi/\partial\mathbf{q}$ is the $m \times n$ Jacobian matrix of the configuration-level constraints, and $\Phi_t = \partial\Phi/\partial t$ is an $m \times 1$ array. Let us further assume that there is another set of \hat{m} constraints whose expression is directly given in terms of the generalized velocities of the system, as

$$\hat{\Phi}(\mathbf{q}, \dot{\mathbf{q}}, t) = \mathbf{A}(\mathbf{q}, t) \dot{\mathbf{q}} + \mathbf{b}(\mathbf{q}, t) = \mathbf{0} \quad (3)$$

where \mathbf{A} is an $\hat{m} \times n$ matrix that will be termed the Jacobian matrix of the velocity-level constraints, and \mathbf{b} is an $\hat{m} \times 1$ array. Such constraints may be introduced in the modelling of the system for convenience reasons (e.g. a constraint relating the angular velocities of two rigid bodies, whose expression at position level may exist but it is not easy to obtain), or because their configuration-level expression does not exist at all. In this latter case, these constraints are called non-holonomic.

The constraint equations introduced in the previous paragraph are combined with the dynamic equations of the system

$$\mathbf{M}\ddot{\mathbf{q}} + \mathbf{c} = \mathbf{Q}_a + \mathbf{Q}_c \quad (4)$$

to fully describe the motion of the constrained system. In Eq. (4), \mathbf{M} stands for the $n \times n$ mass matrix, \mathbf{c} is the array of Coriolis and centrifugal forces, and \mathbf{Q}_a and \mathbf{Q}_c represent the applied forces and the constraint reactions, respectively.

Together, Eqs. (1), (3) and (4) constitute a system of DAE's. Among the different methods available in the multibody systems literature to handle such problems, index-3 augmented Lagrangian formulations represent an efficient and reliable way to carry out the forward-dynamics simulation of constrained mechanical systems, and are currently employed in a wide range of applications (e.g. [1], [2]). Index-3 dynamic equations can be combined with the expressions of a numerical integrator to determine the configuration of the system in the next time-step \mathbf{q}_{k+1} from the values of the generalized positions at time-step k and their time derivatives, e.g. through a Newton-Raphson iteration. Next, the generalized velocities $\dot{\mathbf{q}}_{k+1}$ and accelerations $\ddot{\mathbf{q}}_{k+1}$ at time-step $k+1$ are obtained from \mathbf{q}_{k+1} and the integrator equations. In this last stage, projecting the obtained arrays onto the corresponding constraint manifold is required in order to ensure the satisfaction of the constraints at the velocity and acceleration levels, since only the constraints at position level are enforced in the integration stage.

The index-3 augmented Lagrangian formulation proposed in this paper is based on existing formalisms developed by Bayo and Ledesma [3] and Cuadrado et al. [4]. These algorithms were originally designed to solely handle holonomic constraints and they are unable to solve for non-holonomic constraints and to provide correct values of the reaction forces if the expression of the constraints at the configuration level is not available.

The present work expands the original formulations to cover the case in which some of the kinematic constraints are introduced at the velocity level alone. A new expression of the projection of velocities and accelerations is introduced to impose the satisfaction of the velocity-level constraints, and correct values of the reaction forces associated with them are obtained at the end of the projection process.

2 Expression of the index-3 augmented Lagrangian formulation with the trapezoidal rule as integrator

Following a Lagrangian approach, the constraint reaction forces \mathbf{Q}_c in (4) can be expressed as

$$\mathbf{Q}_c = -\Phi_q^T \boldsymbol{\lambda} - \mathbf{A}^T \hat{\boldsymbol{\lambda}} \quad (5)$$

where $\boldsymbol{\lambda}$ and $\hat{\boldsymbol{\lambda}}$ are the Lagrange multipliers corresponding to the position-level and velocity-level constraints, respectively. Substituting (5) in the dynamic equations (4) results in the expression

$$\mathbf{M}\ddot{\mathbf{q}} = \mathbf{Q} - \Phi_q^T \boldsymbol{\lambda} - \mathbf{A}^T \hat{\boldsymbol{\lambda}} \quad (6)$$

where the term $\mathbf{Q} = \mathbf{Q}_a - \mathbf{c}$ groups both the applied forces and the Coriolis and centrifugal terms. The augmented Lagrangian algorithm described in [3] employs a modified Lagrangian formulation [5], according to which the value of the Lagrange multipliers is proportional to the violation of the constraints at the configuration, velocity, and acceleration levels, via the introduction of penalty factors. The formulation was originally developed for holonomic and non-holonomic constraints. The dynamic equations of the system then become

$$\mathbf{M}\ddot{\mathbf{q}} = \mathbf{Q} - \Phi_q^T \boldsymbol{\alpha} \left(\ddot{\Phi} + 2\xi\omega\dot{\Phi} + \omega^2\Phi \right) - \Phi_q^T \boldsymbol{\lambda}^* - \mathbf{A}^T \hat{\boldsymbol{\alpha}} \left(\dot{\Phi} + \xi\hat{\Phi} \right) - \mathbf{A}^T \hat{\boldsymbol{\lambda}}^* \quad (7)$$

where $\boldsymbol{\alpha}$ and $\hat{\boldsymbol{\alpha}}$ are the $m \times m$ and $\hat{m} \times \hat{m}$ matrices containing the penalty factors associated with the kinematic constraints, and $\boldsymbol{\lambda}^*$ and $\hat{\boldsymbol{\lambda}}^*$ are the Lagrange multipliers of the modified formulation. Terms ξ and ω are scalar parameters for the stabilization of the constraints [6].

Also in [3] the index-3 augmented Lagrangian formulation with projections of velocities and accelerations was developed for holonomic constraints. Following the same ideas of [3], the original formulation can be extended to non-holonomic constraints: a modification of the augmented Lagrangian formulation (7) can be proposed and the terms $\ddot{\Phi}$, $\dot{\Phi}$, $\hat{\Phi}$, and $\hat{\Phi}$ can be dropped from the equation, as they are expected to be eliminated by the projections of velocities and accelerations onto the corresponding constraint manifolds. Moreover, the removal of the violation of velocity-level constraints results in the term $\hat{\boldsymbol{\lambda}}^*$ being zero as well. Then, Eq. (7) takes the form

$$\mathbf{M}\ddot{\mathbf{q}} + \Phi_q^T \boldsymbol{\lambda}^* + \Phi_q^T \boldsymbol{\alpha} \Phi = \mathbf{Q} \quad (8)$$

and the Lagrange multipliers $\boldsymbol{\lambda}^*$ are obtained upon convergence of the iterative process

$$\boldsymbol{\lambda}_{i+1}^* = \boldsymbol{\lambda}_i^* + \boldsymbol{\alpha} \Phi_{i+1}, \quad i = 0, 1, 2, \dots \quad (9)$$

where subscript i stands for the iteration number.

Index-3 augmented Lagrangian formulations deal with Eqs. (8) and (9) by selecting the configuration of the system \mathbf{q} as the primary variable in the numerical integration process during forward-dynamics simulations. However, only the accelerations $\ddot{\mathbf{q}}$ are present in Eq. (8), and the difference equations of a numerical integrator must be used to this end. The implicit, single-step trapezoidal rule integrator is a common choice in the literature (e.g. [7]) and it is used in this work as well. Its expression is a particular case of the Newmark family of integrators [8]

$$\dot{\mathbf{q}}_{k+1} = \frac{\gamma}{\beta h} \mathbf{q}_{k+1} + \hat{\mathbf{q}}_k \tag{10}$$

$$\ddot{\mathbf{q}}_{k+1} = \frac{1}{\beta h^2} \mathbf{q}_{k+1} + \hat{\mathbf{q}}_k \tag{11}$$

$$\hat{\mathbf{q}}_k = - \left[\frac{\gamma}{\beta h} \mathbf{q}_k + \left(\frac{\gamma}{\beta} - 1 \right) \dot{\mathbf{q}}_k + \left(\frac{\gamma}{2\beta} - 1 \right) h \ddot{\mathbf{q}}_k \right] \tag{12}$$

$$\hat{\mathbf{q}}_k = - \left[\frac{1}{\beta h^2} \mathbf{q}_k + \frac{1}{\beta h} \dot{\mathbf{q}}_k + \left(\frac{1}{2\beta} - 1 \right) \ddot{\mathbf{q}}_k \right] \tag{13}$$

where $\beta = 0.25$ and $\gamma = 0.5$, and h stands for the integration time-step. The acceleration at time-step $k + 1$ can be found using Eqs. (10) – (13) as

$$\ddot{\mathbf{q}}_{k+1} = \frac{4}{h} \mathbf{q}_{k+1} + \hat{\mathbf{q}}_k, \quad \text{with} \quad \hat{\mathbf{q}}_k = - \left(\frac{4}{h^2} \mathbf{q}_k + \frac{4}{h} \dot{\mathbf{q}}_k + \ddot{\mathbf{q}}_k \right) \tag{14}$$

Replacing $\ddot{\mathbf{q}}_{k+1}$ in Eq. (8) yields the dynamic equilibrium at time step $k + 1$

$$\mathbf{M} \mathbf{q}_{k+1} + \frac{h^2}{4} \Phi_{\mathbf{q}_{k+1}}^T (\alpha \Phi_{k+1} + \lambda_{k+1}^*) - \frac{h^2}{4} \mathbf{Q}_{k+1} + \frac{h^2}{4} \mathbf{M} \hat{\mathbf{q}}_k = \mathbf{0} \tag{15}$$

where a scaling factor $h^2/4$ has been introduced in order to improve the numerical behaviour of the algorithm. Term $\hat{\mathbf{q}}_k$ comprises only positions, velocities and accelerations at time step k , and is therefore known. Accordingly, Eqs. (15) and (9) constitute a nonlinear system of equations in which \mathbf{q}_{k+1} and λ_{k+1}^* are the unknowns. Such a system can be solved by means of Newton-Raphson iteration

$$\left[\frac{\partial \mathbf{f}(\mathbf{q})}{\partial \mathbf{q}} \right]_i (\mathbf{q}_{i+1} - \mathbf{q}_i) = - [\mathbf{f}(\mathbf{q})]_i \tag{16}$$

where i stands for the iteration number. The right hand side in Eq. (16) is

$$[\mathbf{f}(\mathbf{q})] = \frac{h^2}{4} (\mathbf{M} \ddot{\mathbf{q}} + \Phi_{\mathbf{q}} \alpha \Phi + \Phi_{\mathbf{q}}^T \lambda^* - \mathbf{Q}) \tag{17}$$

and the approximated tangent matrix

$$\left[\frac{\partial \mathbf{f}(\mathbf{q})}{\partial \mathbf{q}} \right] \approx \mathbf{M} + \frac{h}{2} \mathbf{C} + \frac{h^2}{4} (\Phi_{\mathbf{q}}^T \alpha \Phi_{\mathbf{q}} + \mathbf{K}) \tag{18}$$

where

$$\mathbf{K} = - \left(\frac{\partial \mathbf{Q}}{\partial \mathbf{q}} \right); \quad \mathbf{C} = - \left(\frac{\partial \mathbf{Q}}{\partial \dot{\mathbf{q}}} \right) \tag{19}$$

are the so-called stiffness and damping matrices and they represent the contribution of the forces to the derivatives of the residual of Eq. (17). The Lagrange multipliers λ^* in Eq. (9) are also updated during the Newton-Raphson iteration for efficiency reasons. Upon convergence, the iterative process will yield a set of generalized coordinates \mathbf{q}_{k+1} that will satisfy the position-level constraint equations (1), and the values of the reaction forces that correspond to them, λ^* .

3 Projections onto the subspace of admissible motion

The algorithm described in the previous section also provides as a result a set of generalized velocities $\dot{\mathbf{q}}_{k+1}^*$ and another of accelerations $\ddot{\mathbf{q}}_{k+1}^*$. However, these do not necessarily verify the velocity-level constraint equations (2) and (3) nor their time derivatives. In fact, the velocity-level constraints in Eq. (3) have not been imposed at all by the described algorithm. A mass-orthogonal projection method for velocities and accelerations was proposed in [3] to ensure the fulfilment of the velocity and acceleration-level constraint equations. The original method was solely intended to deal with holonomic constraints, and it is expanded in the following sections to handle velocity-level constraints as well. It will be shown that the Lagrange multipliers associated with these represent the reaction forces introduced by the velocity-level constraints.

3.1 Projection of velocities

A set of generalized velocities $\dot{\mathbf{q}}$ that verifies the velocity-level constraints (2) and (3) can be obtained by solving the following minimization problem

$$\begin{aligned} \min V &= \frac{1}{2} (\dot{\mathbf{q}} - \dot{\mathbf{q}}^*)^T \mathbf{P} (\dot{\mathbf{q}} - \dot{\mathbf{q}}^*) \\ \text{s.t. : } c\dot{\Phi}(\mathbf{q}, \dot{\mathbf{q}}, t) &= c(\Phi_{\mathbf{q}}\dot{\mathbf{q}} + \Phi_t) = \mathbf{0} \\ c\hat{\Phi}(\mathbf{q}, \dot{\mathbf{q}}, t) &= c(\mathbf{A}\dot{\mathbf{q}} + \mathbf{b}) = \mathbf{0} \end{aligned} \quad (20)$$

where \mathbf{P} is a symmetric and positive definite projection matrix and c is a scalar constant used to weigh the constraint equations. A way to solve this problem is using an augmented Lagrangian formulation to transform the constrained minimization problem (20) into an equivalent unconstrained one

$$\min_{\dot{\mathbf{q}}} V^* = \frac{1}{2} (\dot{\mathbf{q}} - \dot{\mathbf{q}}^*)^T \mathbf{P} (\dot{\mathbf{q}} - \dot{\mathbf{q}}^*) + \frac{1}{2} c\dot{\Phi}^T \alpha \dot{\Phi} + \dot{\Phi}^T \sigma + \frac{1}{2} c\hat{\Phi}^T \hat{\alpha} \hat{\Phi} + \hat{\Phi}^T \hat{\sigma} \quad (21)$$

where σ and $\hat{\sigma}$ are the Lagrange multipliers of the minimization problem associated with the holonomic and non-holonomic constraints respectively. The same penalty matrices α and $\hat{\alpha}$ of Eq. (7) have been used in Eq. (21), although different values could be used. The necessary condition to obtain the minimum can be expressed as follows

$$\begin{aligned} \frac{\partial V^*}{\partial \dot{\mathbf{q}}} &= \mathbf{P} (\dot{\mathbf{q}} - \dot{\mathbf{q}}^*) + c\dot{\Phi}_{\mathbf{q}}^T \alpha \dot{\Phi} + \dot{\Phi}_{\mathbf{q}}^T \sigma + c\mathbf{A}^T \hat{\alpha} \hat{\Phi} + \mathbf{A}^T \hat{\sigma} \\ &= \mathbf{P} (\dot{\mathbf{q}} - \dot{\mathbf{q}}^*) + c\dot{\Phi}_{\mathbf{q}}^T \alpha (\Phi_{\mathbf{q}}\dot{\mathbf{q}} + \Phi_t) + \dot{\Phi}_{\mathbf{q}}^T \sigma + c\mathbf{A}^T \hat{\alpha} (\mathbf{A}\dot{\mathbf{q}} + \mathbf{b}) + \mathbf{A}^T \hat{\sigma} = \mathbf{0} \end{aligned} \quad (22)$$

Expression (22) is a nonlinear system of equations that can be solved via fixed-point iteration

$$(\mathbf{P} + c\dot{\Phi}_{\mathbf{q}}^T \alpha \Phi_{\mathbf{q}} + c\mathbf{A}^T \hat{\alpha} \mathbf{A}) \dot{\mathbf{q}}_{i+1} = \mathbf{P}\dot{\mathbf{q}}^* - c\dot{\Phi}_{\mathbf{q}}^T \alpha \Phi_t - \dot{\Phi}_{\mathbf{q}}^T \sigma_{i+1} - c\mathbf{A}^T \hat{\alpha} \mathbf{b} - \mathbf{A}^T \hat{\sigma}_{i+1} \quad (23)$$

$$\sigma_{i+1} = \sigma_i + c\alpha \dot{\Phi} \quad (24)$$

$$\hat{\sigma}_{i+1} = \hat{\sigma}_i + c\hat{\alpha} \hat{\Phi} \quad (25)$$

yielding the set of velocities $\dot{\mathbf{q}}$.

3.2 Projection of accelerations

The set of accelerations $\ddot{\mathbf{q}}^*$ can be projected onto the subspace of admissible motion following a similar approach. The problem to solve for the accelerations is the following one

$$\begin{aligned} \min V &= \frac{1}{2} (\ddot{\mathbf{q}} - \ddot{\mathbf{q}}^*)^T \mathbf{P} (\ddot{\mathbf{q}} - \ddot{\mathbf{q}}^*) \\ \text{s.t. : } c\ddot{\Phi}(\mathbf{q}, \dot{\mathbf{q}}, \ddot{\mathbf{q}}, t) &= c(\Phi_{\mathbf{q}}\ddot{\mathbf{q}} + \dot{\Phi}_{\mathbf{q}}\dot{\mathbf{q}} + \ddot{\Phi}_t) = \mathbf{0} \\ c\hat{\ddot{\Phi}}(\mathbf{q}, \dot{\mathbf{q}}, \ddot{\mathbf{q}}, t) &= c(\mathbf{A}\ddot{\mathbf{q}} + \dot{\mathbf{A}}\dot{\mathbf{q}} + \mathbf{b}) = \mathbf{0} \end{aligned} \quad (26)$$

where $\ddot{\mathbf{q}}$ is a set of accelerations that fulfills the time derivatives of constraint equations (2) and (3). The use of the augmented Lagrangian method transforms the constrained problem (26) into

$$\min_{\ddot{\mathbf{q}}} V^* = \frac{1}{2} (\ddot{\mathbf{q}} - \ddot{\mathbf{q}}^*)^T \mathbf{P} (\ddot{\mathbf{q}} - \ddot{\mathbf{q}}^*) + \frac{1}{2} c\ddot{\Phi}^T \alpha \ddot{\Phi} + \ddot{\Phi}^T \kappa + \frac{1}{2} c\hat{\ddot{\Phi}}^T \hat{\alpha} \hat{\ddot{\Phi}} + \hat{\ddot{\Phi}}^T \hat{\kappa} \quad (27)$$

where κ and $\hat{\kappa}$ are the Lagrange multipliers of the minimization problem for the position-level and velocity-level constraints, respectively. Imposing the condition for the existence of a minimum

$$\begin{aligned} \frac{\partial V^*}{\partial \ddot{\mathbf{q}}} &= \mathbf{P} (\ddot{\mathbf{q}} - \ddot{\mathbf{q}}^*) + c\ddot{\Phi}_{\mathbf{q}}^T \alpha \ddot{\Phi} + \ddot{\Phi}_{\mathbf{q}}^T \kappa + c\mathbf{A}^T \hat{\alpha} \hat{\ddot{\Phi}} + \mathbf{A}^T \hat{\kappa} \\ &= \mathbf{P} (\ddot{\mathbf{q}} - \ddot{\mathbf{q}}^*) + c\ddot{\Phi}_{\mathbf{q}}^T \alpha (\Phi_{\mathbf{q}}\ddot{\mathbf{q}} + \dot{\Phi}_{\mathbf{q}}\dot{\mathbf{q}} + \ddot{\Phi}_t) + \ddot{\Phi}_{\mathbf{q}}^T \kappa \\ &\quad + c\mathbf{A}^T \hat{\alpha} (\mathbf{A}\ddot{\mathbf{q}} + \dot{\mathbf{A}}\dot{\mathbf{q}} + \mathbf{b}) + \mathbf{A}^T \hat{\kappa} = \mathbf{0} \end{aligned} \quad (28)$$

and solving with fixed-point iteration

$$(\mathbf{P} + c\Phi_{\mathbf{q}}^T \alpha \Phi_{\mathbf{q}} + c\mathbf{A}^T \hat{\alpha} \mathbf{A}) \ddot{\mathbf{q}}_{i+1} = \mathbf{P} \ddot{\mathbf{q}}^* - c\Phi_{\mathbf{q}}^T \alpha (\dot{\Phi}_{\mathbf{q}} \dot{\mathbf{q}} + \dot{\Phi}_t) - \Phi_{\mathbf{q}}^T \kappa_{i+1} - c\mathbf{A}^T \hat{\alpha} (\dot{\mathbf{A}} \dot{\mathbf{q}} + \mathbf{b}) - \mathbf{A}^T \hat{\kappa}_{i+1} \quad (29)$$

$$\kappa_{i+1} = \kappa_i + c\alpha \ddot{\Phi} \quad (30)$$

$$\hat{\kappa}_{i+1} = \hat{\kappa}_i + c\hat{\alpha} \dot{\hat{\Phi}} \quad (31)$$

yields the set of accelerations $\ddot{\mathbf{q}}$.

3.3 Selection of the projection matrix

There is a number of possibilities to select the projection matrix \mathbf{P} and the scalar constant c . The choice strongly affects the behaviour of the projection algorithm. In the case of the velocity projections, the selection has a useful physical meaning in terms of energy dissipation, as it was described in [9]. Two alternatives have been explored in this work:

1. The original projections introduced by Bayo and Ledesma [3]: $\mathbf{P} = \mathbf{M}$, $c = 1$. It was proved in [9] that this selection introduces unconditional dissipation to any incompatible velocity field in the velocity projections, which produces a very stable behaviour.
2. The modified projections of Cuadrado et al. [4]: $\mathbf{P} = \mathbf{M} + h/2 \mathbf{C} + h^2/4 \mathbf{K}$, $c = h^2/4$. This choice was intended to make the leading matrix of the projections of velocities and accelerations in Eqs. (23) and (29) equal to the approximate tangent matrix of the Newton-Raphson iteration (18). Therefore, the factorization of the tangent matrix, carried out to solve system (16) could be used during the projection step. The consideration of velocity-level constraints, however, introduces a new term $c\mathbf{A}^T \hat{\alpha} \mathbf{A}$ in the leading matrix of the projections that needs to be accounted for.

4 Calculation of the constraint reactions from the projection stage

The projection step described in Section 3 modifies the velocities and accelerations yielded by the Newton-Raphson iteration in order to make them fulfil the sets of constraints (2) and (3). For those constraints with a readily available expression at the position level (1), the projection step removes the violation of the constraints at velocity and acceleration levels that arises due to inaccuracies in the integration method. The Newton-Raphson iteration (16), however, takes care of imposing the constraints at the position level, and so the reaction forces associated with them are represented by the Lagrange multipliers λ^* of the iterative process. This is not the case of those constraints defined only at the velocity-level (3), which are enforced by the projection step alone. The reaction forces associated with these constraints can be obtained either from the projection of velocities or from the projection of accelerations.

The projection step transforms the set of accelerations of the system $\ddot{\mathbf{q}}^*$ into $\ddot{\mathbf{q}}$. This is equivalent to exerting a force

$$\mathbf{Q}^{proj} = \mathbf{M}(\ddot{\mathbf{q}} - \ddot{\mathbf{q}}^*) \quad (32)$$

on the system. For the Bayo and Ledesma projections ($\mathbf{P} = \mathbf{M}$, $c = 1$), Eqs. (29)–(31) corresponding to the projection of accelerations take the form

$$(\mathbf{M} + \Phi_{\mathbf{q}}^T \alpha \Phi_{\mathbf{q}} + \mathbf{A}^T \hat{\alpha} \mathbf{A}) \ddot{\mathbf{q}} = \mathbf{M} \ddot{\mathbf{q}}^* - \Phi_{\mathbf{q}}^T \alpha (\dot{\Phi}_{\mathbf{q}} \dot{\mathbf{q}} + \dot{\Phi}_t) - \Phi_{\mathbf{q}}^T \kappa_{i+1} - \mathbf{A}^T \hat{\alpha} (\dot{\mathbf{A}} \dot{\mathbf{q}} + \mathbf{b}) - \mathbf{A}^T \hat{\kappa}_{i+1} \quad (33)$$

$$\kappa_{i+1} = \kappa_i + \alpha \ddot{\Phi} \quad (34)$$

$$\hat{\kappa}_{i+1} = \hat{\kappa}_i + \hat{\alpha} \dot{\hat{\Phi}} \quad (35)$$

The reaction force introduced by the projections can be obtained from Eqs. (32) and (33) as

$$\begin{aligned} \mathbf{Q}^{proj} &= -\Phi_{\mathbf{q}}^T \alpha (\Phi_{\mathbf{q}} \ddot{\mathbf{q}} + \dot{\Phi}_{\mathbf{q}} \dot{\mathbf{q}} + \dot{\Phi}_t) - \Phi_{\mathbf{q}}^T \kappa_{i+1} - \mathbf{A}^T \hat{\alpha} (\mathbf{A} \ddot{\mathbf{q}} + \dot{\mathbf{A}} \dot{\mathbf{q}} + \mathbf{b}) - \mathbf{A}^T \hat{\kappa}_{i+1} \\ &= -\Phi_{\mathbf{q}}^T (\alpha \ddot{\Phi} + \kappa_{i+1}) - \mathbf{A}^T (\hat{\alpha} \dot{\hat{\Phi}} + \hat{\kappa}_{i+1}) \end{aligned} \quad (36)$$

Similarly, for the projection of velocities of Eqs. (23)–(25)

$$(\mathbf{M} + \Phi_{\mathbf{q}}^T \alpha \Phi_{\mathbf{q}} + \mathbf{A}^T \hat{\alpha} \mathbf{A}) \dot{\mathbf{q}} = \mathbf{M} \dot{\mathbf{q}}^* - \Phi_{\mathbf{q}}^T \alpha \Phi_t - \Phi_{\mathbf{q}}^T \sigma_{i+1} - \mathbf{A}^T \hat{\alpha} \mathbf{b} - \mathbf{A}^T \hat{\sigma}_{i+1} \quad (37)$$

$$\sigma_{i+1} = \sigma_i + \alpha \dot{\Phi} \quad (38)$$

$$\hat{\sigma}_{i+1} = \hat{\sigma}_i + \hat{\alpha} \dot{\hat{\Phi}} \quad (39)$$

The following relation between velocities and accelerations holds for the trapezoidal rule used as integrator

$$\dot{\mathbf{q}}_{k+1} = \dot{\mathbf{q}}_k + \frac{h}{2} (\ddot{\mathbf{q}}_k + \ddot{\mathbf{q}}_{k+1}) \quad (40)$$

Substituting Eq. (40) in Eq. (37)

$$\begin{aligned} & (\mathbf{M} + \Phi_{\mathbf{q}}^T \alpha \Phi_{\mathbf{q}} + \mathbf{A}^T \hat{\alpha} \mathbf{A}) \left(\dot{\mathbf{q}}_k + \frac{h}{2} (\ddot{\mathbf{q}}_k + \ddot{\mathbf{q}}_{k+1}) \right) = \\ & \mathbf{M} \left(\dot{\mathbf{q}}_k + \frac{h}{2} (\ddot{\mathbf{q}}_k + \ddot{\mathbf{q}}_{k+1}^*) \right) - \Phi_{\mathbf{q}}^T \alpha \Phi_{\mathbf{t}} - \Phi_{\mathbf{q}}^T \sigma_{i+1} - \mathbf{A}^T \hat{\alpha} \mathbf{b} - \mathbf{A}^T \hat{\sigma}_{i+1} \end{aligned} \quad (41)$$

and so it is possible to obtain the forces introduced by the projection from the velocity-level expression as

$$\mathbf{Q}^{proj} = \mathbf{M} (\ddot{\mathbf{q}} - \ddot{\mathbf{q}}^*) = -\frac{2}{h} \left(\Phi_{\mathbf{q}}^T (\alpha \hat{\Phi} + \sigma_{i+1}) + \mathbf{A}^T (\hat{\alpha} \hat{\Phi} + \hat{\sigma}_{i+1}) \right) \quad (42)$$

Finally, the total constraint reaction force acting on the system, considering the contribution of both the Newton-Raphson iteration and the projection step is given by the following expression

$$\mathbf{Q}_c = \Phi_{\mathbf{q}}^T (\alpha \lambda_{i+1}^*) + \mathbf{Q}^{proj} \quad (43)$$

where the term \mathbf{Q}^{proj} can be obtained from either Eq. (36) or (42).

5 Numerical examples

The method to evaluate the constraint reaction forces described in Section 4 was assessed in the forward-dynamics simulation of a set of simple examples with known analytical solutions.

The first test problem consisted of two point masses linked by a velocity constraint that specifies their relative velocity in the x direction, shown in Fig. 1.

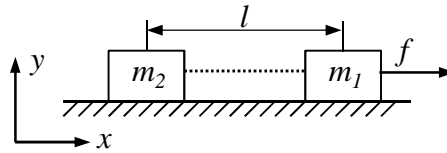


Figure 1. Velocity constraint in the x direction acting between two point masses

If the constraint establishes that the relative velocity between the two point masses is zero ($\dot{x}_1 - \dot{x}_2 = 0$), then the value of the reaction force f_c exerted by the constraint can be evaluated as

$$f_c = \frac{f m_2}{m_1 + m_2} \quad (44)$$

The original algorithms described in [3] and [4] correctly determine the value of the reaction force if the constraint is expressed at the position level ($x_1 - x_2 - l = 0$). However, they are unable to provide the value of f_c when the constraint is defined at the velocity level; as no position-level constraints exist, there are no Lagrange multipliers λ^* in Eq. (8). The general formulation introduced in this work was used to obtain the reaction force from Eq. (43). A 5 s forward-dynamics simulation was carried out selecting as particular values of the parameters of the system $m_1 = 7$ kg, $m_2 = 5$ kg, $l = 3$ m, and $f = 2$ N. The projection matrix was set to $\mathbf{P} = \mathbf{M}$, the coefficient $c = 1$, and the penalty factor for the constraint equation was $\alpha = 10^6$. The integration time-step was set to $h = 10^{-3}$ s and the limit of iterations for both the Newton-Raphson convergence and the projections was fixed to 10. With these parameters, the reaction force was computed with Eq. (43), either using the reaction forces \mathbf{Q}^{proj} yielded by the projection of accelerations with Eq. (36) or the ones from the projection of velocities with Eq. (42). In both cases, the result was $f_c = 0.833$ N, which is the value theoretically predicted with (44).

The second example consisted of two point masses moving on the xy plane (Fig. 2). The motion of this system was described with four generalized coordinates x_A , y_A , x_B , and y_B . In this case, the velocity of the mass at point A is

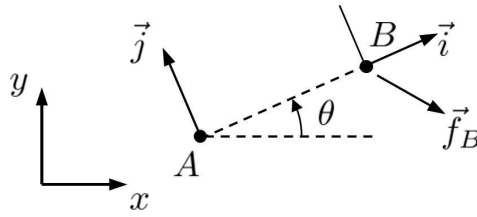


Figure 2. Non-holonomic constraint restraining the velocity of mass A to be collinear with segment $A - B$

constrained to be pointing towards B at every instant by the velocity-level constraint $(y_B - y_A) \dot{x}_A - (x_B - x_A) \dot{y}_A = 0$. It can be shown that this constraint is non-holonomic, since no equivalent position-level expression can be found for it. Both masses are initially moving with constant velocity $\dot{x}_A = \dot{x}_B = 1$ m/s, while $\dot{y}_A = \dot{y}_B = 0$. A force $f_B = 2$ N is acting in the vertical direction on point B . A 5 s long forward-dynamics simulation was carried out with the described system of masses, using two different methods to solve the dynamic equations. The first one was the direct solution of the system resulting from expressing Eq. (4) with a Lagrangian formulation, establishing $\mathbf{Q}_c = -\mathbf{A}^T \hat{\lambda}$

$$\begin{bmatrix} \mathbf{M} & \mathbf{A}^T \\ \mathbf{A} & \mathbf{0} \end{bmatrix} \begin{bmatrix} \ddot{\mathbf{q}} \\ \hat{\lambda} \end{bmatrix} = \begin{bmatrix} \mathbf{Q} \\ -\dot{\mathbf{A}}\dot{\mathbf{q}} - 2\xi\omega\hat{\Phi} \end{bmatrix} \tag{45}$$

The trapezoidal rule was used as integrator, with an integration time-step $h = 10^{-3}$ s.

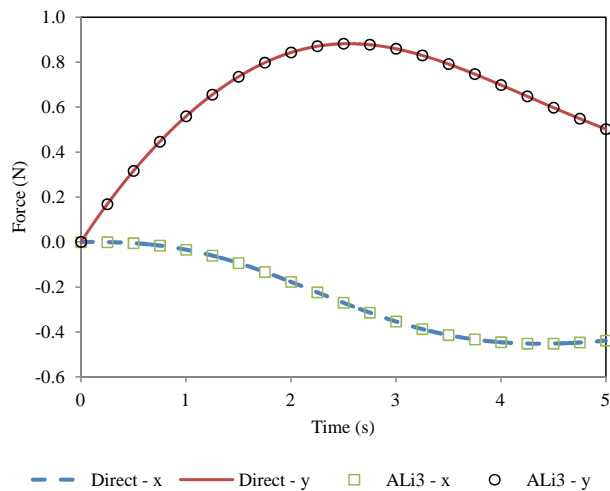


Figure 3. Reaction forces acting on mass A in the x and y directions due to the non-holonomic constraint in the second example, computed with direct solution (Eq. (45)) and with the index-3 formulation with projections

Second, the simulation was repeated with the same parameters using the index-3 augmented Lagrangian formulation with $\mathbf{P} = \mathbf{M}$ and $c = 1$. The reaction forces associated with the non-holonomic constraint were evaluated using the results of the projection process as described in Section 4. Results are shown in Fig. 3. The direct solution method and the augmented Lagrangian formulation yielded the same constraint reaction forces. Moreover, the obtained results with the Lagrangian formulation were the same, regardless of whether the reaction forces were obtained from the projection of accelerations with Eq. (36) or from the projection of velocities with Eq. (42).

The last test problem is a three-dimensional rigid wheel rolling on a horizontal plane (Fig. 4). This system was modelled using a set of 12 natural coordinates [10], restrained by a set of constraint equations, defined both at the position and the velocity levels. The set of natural coordinates comprised the x , y and z coordinates of the center of the wheel (P) and three unit vectors \vec{u} , \vec{v} , and \vec{w} that form the local reference frame of the wheel. At time $t = 0$ s, vectors \vec{u} , \vec{v} , and \vec{w} are aligned with the inertial reference frame x , y , z . Six kinematic constraints were introduced to enforce that the set of coordinates behaves as a rigid body. The norm of vectors \vec{u} , \vec{v} , and \vec{w} was constrained to be 1, and the angles between them were made constant during motion. Moreover, the wheel was constrained to roll on the ground plane via

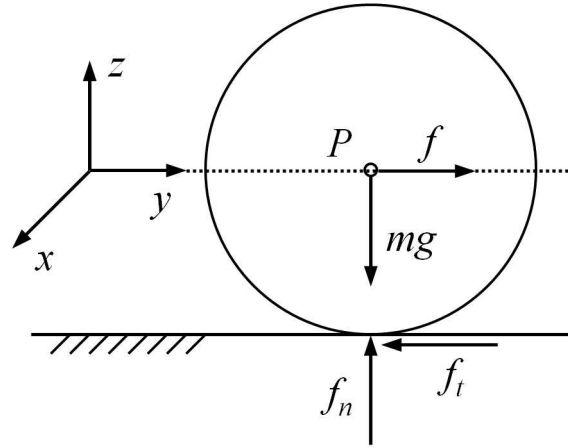


Figure 4. Wheel rolling on a plane

the introduction of four kinematic constraints. The first one was a configuration-level constraint to keep constant the distance between point P and the ground. If the equation of the ground plane in the inertial reference frame is given by $n_a x + n_b y + n_c z + n_d = 0$, this is achieved with the constraint

$$|n_a r_{px} + n_b r_{py} + n_c r_{pz} + n_d| - r \sqrt{n_a^2 + n_b^2 + n_c^2} = 0 \quad (46)$$

where r_{px} , r_{py} , and r_{pz} are the x , y , and z components of the position vector of point P , \mathbf{r}_P , and r is the wheel radius. Moreover, defining the 3×3 matrix

$$\mathbf{X} = [\mathbf{u} \quad \mathbf{v} \quad \mathbf{w}] \quad (47)$$

where \mathbf{u} , \mathbf{v} , and \mathbf{w} are the arrays of generalized coordinates associated with vectors \vec{u} , \vec{v} , and \vec{w} , allows writing the skew-symmetric matrix associated with the angular velocity of the wheel as [11]

$$\tilde{\omega} = \dot{\mathbf{X}}\mathbf{X}^T \quad (48)$$

The rolling condition for the wheel when the camber angle is 0 can be expressed as

$$\dot{\mathbf{r}}_P - r \tilde{\mathbf{X}}\mathbf{X}^T \mathbf{n} = \mathbf{0} \quad (49)$$

where \mathbf{n} is the normal to the ground plane. Eq. (49) introduces three velocity-level equations in the set of kinematic constraints, which in general cannot be reduced to an equivalent configuration-level expression.

The wheel moves under gravity effects and the action of a horizontal force of magnitude f acting on the positive direction of the y axis. The resultant motion is a planar rolling contained in the zy plane. The imposition of rolling introduces two reaction forces with magnitudes f_n and f_t in the normal and tangent directions at the contact point, respectively. While the normal force can be obtained with traditional index-3 formulations, as it is introduced by the position-level constraint (46), reaction f_t is generated by the rolling condition (49) and it cannot be found with the existing algorithms.

A 5 s forward-dynamics simulation of the motion of the wheel was carried out selecting as particular values for the wheel parameters $m = 2.5467$ kg, $r = 0.175$ m, and $I_{xx} = 0.045224$ kgm². The value of the applied force was set to $f = 2$ N between $t = 1.5$ s and $t = 2.5$ s, and to $f = 0$ N during the rest of the motion. With these values, the reaction force f_t can be determined using the free body diagram of the wheel. Its value is $f_t = 0.734$ N between $t = 1.5$ s and $t = 2.5$ s, and $f_t = 0$ N otherwise. Eqs. (36) and (42) were used to evaluate f_t during the simulation.

Figure 5 shows the value of f_t obtained with the projection method. The results obtained from the projection of accelerations and velocities were almost identical, and the difference between the two of them remained smaller than $3 \cdot 10^{-6}$ N.

6 Conclusions

Existing index-3 augmented Lagrangian formalisms were not designed to tackle kinematic constraints defined at the velocity level alone. In particular, the calculation of the reaction forces associated with this kind of constraints was not

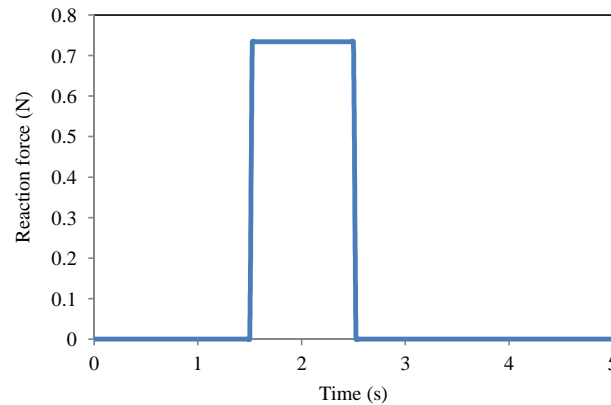


Figure 5. Tangent reaction force f_t during motion of the single wheel.

possible, as the Lagrange multipliers in these algorithms depend only on the violation of constraints at the configuration level. In this work, a simple and efficient technique to obtain the reaction forces introduced by velocity-level constraints was presented. Such reaction forces are computed via a modification of the projection of velocities and accelerations onto the subspace of admissible motion, a step that was already present in the original algorithms. Results obtained from the forward-dynamics simulation of simple examples showed that the method is able to yield correct values of the reaction forces associated with velocity-level constraints, including non-holonomic ones.

References

- [1] F. González, M. A. Naya, A. Luaces, and M. González. On the effect of multirate co-simulation techniques in the efficiency and accuracy of multibody system dynamics. *Multibody System Dynamics*, 25(4):461 – 483, 2011.
- [2] D. Dopico, A. Luaces, M. González, and J. Cuadrado. Dealing with multiple contacts in a human-in-the-loop application. *Multibody System Dynamics*, 25(2):167–183, 2011.
- [3] E. Bayo and R. Ledesma. Augmented Lagrangian and mass–orthogonal projection methods for constrained multibody dynamics. *Nonlinear Dynamics*, 9(1-2):113–130, 1996.
- [4] J. Cuadrado, J. Cardenal, P. Morer, and E. Bayo. Intelligent simulation of multibody dynamics: Space–state and descriptor methods in sequential and parallel computing environments. *Multibody System Dynamics*, 4(1):55–73, 2000.
- [5] E. Bayo, J. García de Jalón, and M. A. Serna. A modified Lagrangian formulation for the dynamic analysis of constrained mechanical systems. *Computer Methods in Applied Mechanics and Engineering*, 71(2):183–195, 1988.
- [6] J. Baumgarte. Stabilization of constraints and integrals of motion in dynamical systems. *Computer Methods in Applied Mechanics and Engineering*, 1:1–16, 1972.
- [7] J. Cuadrado, D. Dopico, M. A. Naya, and M. González. Penalty, semi-recursive and hybrid methods for MBS real-time dynamics in the context of structural integrators. *Multibody System Dynamics*, 12(2):117–132, 2004.
- [8] N. M. Newmark. A method of computation for structural dynamics. *Journal of the Engineering Mechanics Division, ASCE*, 85(EM3):67–94, 1959.
- [9] J. C. García Orden and D. Dopico. *Multibody Dynamics. Computational Methods and Applications*, chapter On the Stabilizing Properties of Energy-Momentum Integrators and Coordinate Projections for Constrained Mechanical Systems, pages 49–67. Springer, 2007.
- [10] J. García de Jalón and E. Bayo. *Kinematic and Dynamic Simulation of Multibody Systems. The Real–Time Challenge*. Springer–Verlag, 1994.
- [11] J. García de Jalón and A. Callejo. A straight methodology to include multibody dynamics in graduate and undergraduate subjects. *Mechanism and Machine Theory*, 46(2):168–182, 2011.

